JOURNAL OF PHYSICAL ORGANIC CHEMISTRY
J. Phys. Org. Chem. 2006; **19:** 53–60
Published online 21 October 2005 in Wiley InterScience (www.interscience.wiley.com). DOI: 10.1002/poc.995

Understanding self-organization of the inclusion complexes in the solid state—DSC, NMR and DFT studies

M. J. Potrzebowski,* J. Heliński, S. Olejniczak and W. Ciesielski

Department of Structural Studies of the Centre of Molecular and Macromolecular Studies, Polish Academy of Sciences, Sienkiewicza 112, PL-90-363 Łódź, Poland

Received 20 May 2005; revised 6 July 2005; accepted 9 August 2005

ABSTRACT: The relationship between DSC profiles and changes of ^{13}C and ^{31}P the spin–lattice relaxation time of the host and ^{1}H T_1 of guest in inclusion complexes of bis[6-*O*,6-*O*′-(1,2:3,4-diisopropylidene-α-D-galactopyranosyl)thiophosphoryl] disulfide (DGTD) with *n*-propanol is discussed in term of guest migration in the crystal lattice. ^{1}H–^{13}C FSLG HETCOR experiment recorded with different contact times was employed to establish the guest localization in the crystal lattice for different modifications of the inclusion complex. The migration pathway of the guest was verified by means of theoretical DFT calculations. Copyright © 2005 John Wiley & Sons, Ltd.
Supplementary electronic material for this paper is available in Wiley Interscience at http://www.interscience.wiley.com/jpages/0894-3230/suppmat/

KEYWORDS: ^{1}H magic angle spinning; ^{1}H–^{13}C FSLG HECTOR; inclusion complexes; solid-state NMR; T_1 relaxation time; thiophosphate

INTRODUCTION

Inclusion complexes (ICs) are attractive models for searching for the mechanism of molecular recognition and for the investigation of the nature of intermolecular contacts.[1] The recognition phenomena in chemistry and biology involve such interactions as electrostatic, van der Waals, hydrophobic, hydrogen bonding, charge transfer, π–π stacking interactions and steric effects.[2,3] A wide variety of experimental methods have been employed to investigate subtle structural effects in ICs at both the macroscopic and molecular levels. A complementary approach which provides the bridge between these two levels is of particular interest.

There are number of organic host molecules which are commonly used to search for host–guest interactions. Natural cyclodextrins consisting of at least 6–8 glucopyranoside rings belong to the class of the most important host molecules owing their ability to incorporate selectively many organic and inorganic molecules, ions and even radicals.[4] Another group of significant host molecules is represented by cyclophosphazene derivatives with a phosphorus atom in the central part of host.[5] The attraction of phosphazenes is due to their wide range of applications in fields such as medicine, flame retardancy and microlithography.

In this paper, we present results for inclusion complexes formed by bis[6-*O*,6-*O*′-(1,2:3,4-diisopropylidene-α-D-galactopyranosyl)thiophosphoryl] disulfide (DGTD) (**1**, Chart 1) host molecule, for which the building units consist of sugar residues and phosphorus atoms. Employing DFT, DSC and solid-state NMR studies, we demonstrated that a consistent insight into self-organization of ICs can be gained with a multi-technique approach. In this work, we used a DGTD•*n*-propanol assembly as a model complex with established x-ray structure for one of the modifications.[6]

RESULTS

DSC and TGA studies

Differential scanning calorimetry (DSC) is frequently a preferred analytical technique because of its ability to provide detailed macroscopic information about both the physical and energetic properties of substances.[7] Figure 1 shows the DSC curves for samples crystallized from *n*-propanol under slightly different conditions (see Experimental for details). For modification **1a** [Fig. 1(a)], one exothermic and two endothermic peaks are seen, whereas **1b** shows a slightly different DSC profile, where the exothermic peak is not so sharp and intense [Fig. 1(b)]. For **1c**, a rather broad exothermic profile is observed. The sharp peak at 109.53 °C

**Correspondence to:* M. J. Potrzebowski, Department of Structural Studies of the Centre of Molecular and Macromolecular Studies, Polish Academy of Sciences, Sienkiewicza 112, PL-90-363 Łódź, Poland.
E-mail: marekpot@bilbo.cbmm.lodz.pl

Contract/grant sponsor: Committee for Scientific Research (MIiN);
Contract/grant number: 3 T09 A 173 27.

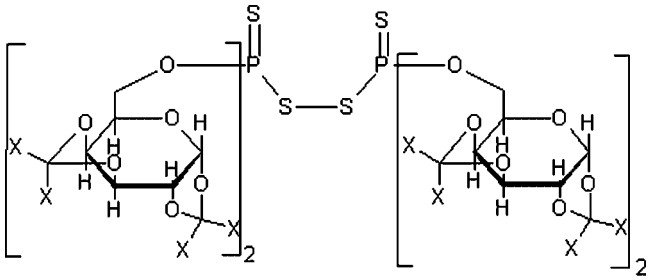

Chart 1

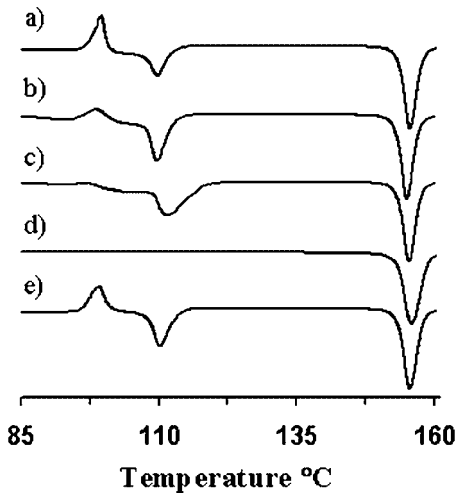

Figure 1. DSC profiles of inclusion complexes of **1** with *n*-propanol inside lattice (a–c). Trace (d) represents homomolecular sample without solvent in lattice. Trace (e) shows profile of modifications **b** and **c** kept at ambient temperature 2 months. Only the region of interest is shown

corresponds to solvent release from the lattice. The endothermic peak at 156.05 °C represents melting temperature of samples. The fourth modification (**1d**) represents a homomolecular system that has not included a solvent molecule in the crystal lattice during the crystallization process. For **1d**, only an endothermic peak (melting-point) is seen. Thermogravimetric analysis of **1a**–**c** confirms the presence of *n*-propanol in the lattice (see Supplementary material, available in Wiley Interscience).

Their yields are very similar (~8%) and correspond to theoretical values calculated from x-ray data. The most interesting results were noted on repeating DSC measurements for samples kept at room temperature for 2 months. Figure 1(e) shows the DSC profile of **1b** and **c** with a clear exothermic peak. This curve is very similar to that observed for **1a**. The DSC of **1a** and **d** after 2 months does not show changes.

The challenge is to rationalize this observation on the molecular level. The method of choice, which allows the investigation of all material, not just an arbitrary selected part of a sample (e.g. x-ray of a single crystal), is high-resolution solid-state NMR of powders.[8]

^{13}C and ^{31}P CP/MAS NMR of host molecule

Figure 2 presents ^{31}P cross-polarization magic angle spinning (CP/MAS) spectra of complexes with *n*-propanol (**1a–c**) and host matrix **1d** without solvent. The difference between the spectra for samples with and without solvent is apparent. In contrast, the ^{31}P CP/MAS spectra of **1–c** are similar. The principal components δ_{ii} of the ^{31}P CST calculated from the spinning sideband intensities using the SIMPSON program[9] are also very similar (see Supplementary material). The ^{13}C CP/MAS spectra for modifications **1a–c** show only minute differences, whereas that of **1d** is considerably different (Fig. 3). It was found that the diagnostic and sensitive NMR parameters that correlate very well with DSC profiles is the spin–lattice relaxation times, ^{31}P T_1 and ^{13}C T_1, of anomeric carbons (Table 1).[10] For **1a** the ^{31}P T_1 is shortest, whereas for **1c** it is about eight times longer and comparable to that of without solvent in the lattice. For **1b,** ^{31}P T_1 is between those for **1a** and **1c**. For samples **1b** and **c** kept at room temperature, the relaxation times gradually decrease, reaching the value for **1a**. These changes are consistent with the changes in the DSC curves [Fig. 1(e)] and show a simple relationship, with larger exothermic peaks with shorter relaxation times. Our results clearly prove that the presence of a solvent molecule inside the crystal lattice has a significant influence on the relaxation parameters of the host

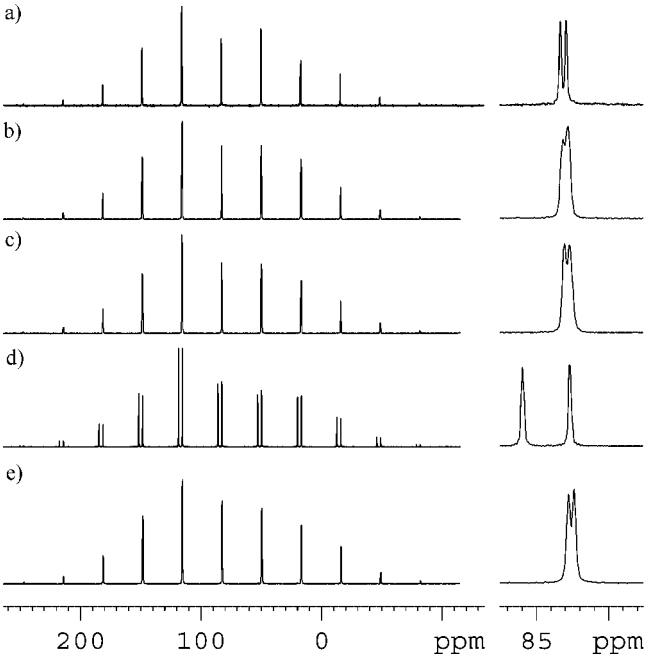

Figure 2. ^{31}P CP/MAS spectra of modifications **1a–e** recorded with a spinning rate of 4 kHz. The right column shows the expanded isotropic part of the spectra

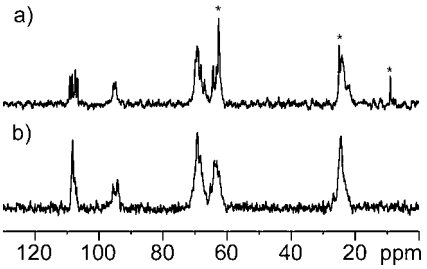

Figure 3. ^{13}C CP/MAS spectra of modifications **1a** (a) and **d** (b) recorded with a spinning rate of 10 kHz. Asterisks denote *n*-propanol signals in the lattice

Table 1. ^{13}C and ^{31}P T_1 relaxation times of different modifications of DGTD•*n*-propanol[a]

	Sample				
	1a (2a)	**1b**	**1c (2c)**	**1d**	**1e**
^{31}P T_1 (s)	14.8	38.0	115.0	114.8	15.0
^{13}C T_1 (s)	15.2	32.2	36.1	79.1	18.5
	34.0	35.0	46.1	80.0	41.0

[a] **1d** represents solvent-free host matrix. For ^{13}C T_1 only anomeric carbons are shown.

(see **1a** and **d**). Comotti *et al.* reported similar observations for cyclophosphazene derivatives.[11] They concluded that a solvent-free matrix is more rigid, hence ^{13}C T_1 relaxation times are longer. However, the question of what the influence of the guest on the relaxation time of the host is remains open. We assume that host–guest interaction is an important mechanism for the relaxation rate R_1 and at least three factors, $R_1 = R_{1CSA} + R_{1DD} + R_{1Guest}$, should be taken into consideration. If this assumption is valid, the localization of the solvent and close proximity to a particular center of the host will be critical factors contributing to overall relaxation. Thus for **1a–c** ICs we predict that during crystallization we have two kinds of crystals with exactly the same geometry of the host but different orientations of the guests.

^{1}H NMR and ^{1}H–^{13}C FSLG HETCOR NMR studies of host–guest interactions

So far, the inclusion complexes of **1** were studied by inspection of the spectral parameters of the host molecule. In this section, we present NMR data for guest species. The localization of *n*-propanol in the crystal cavity of **1a** is known from x-ray studies of single crystals. As shown in Fig. 4(a), the *n*-propanol is located around parallel columns. The guest molecules are kept in channels in which isopropylidene methyl groups are directed to the inside of channels causing steric hindrance. The shortest distances between the host and guest are presented in Fig. 4(b). In order to establish the

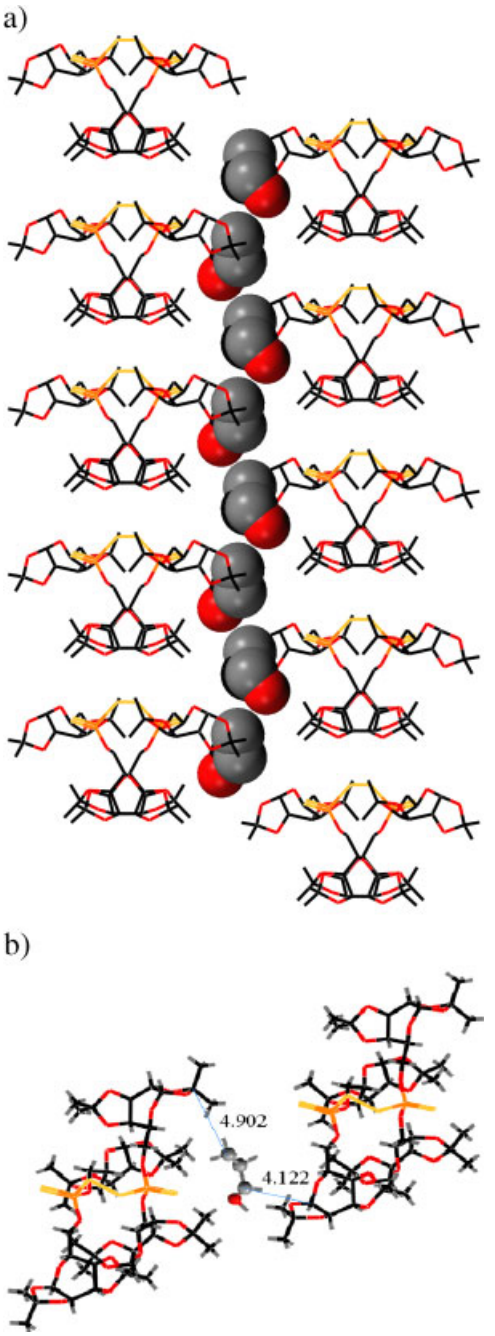

Figure 4. (a) Molecular packing of host–guest in inclusion complex of **1a**. Guest is shown as spacefill and host as stick models. (b) Distances between guest and host in the crystal lattice. Data are taken from Ref. 6 (This figure is available in colour online)

correlation between the structure of the IC and NMR spectral parameters we carried out ^{1}H MAS measurements. Figure 5(a) displays the spectrum of **1a** recorded with a spinning speed 30 kHz at 278 K. The spectrum presents two kinds of proton signals. We assume that the very broad line represents protons which belong to sugar molecules whereas very sharp signals characterize the *n*-propanol. However, in this assumption it is not clear what the contribution of the methyl signals of isopropylidene

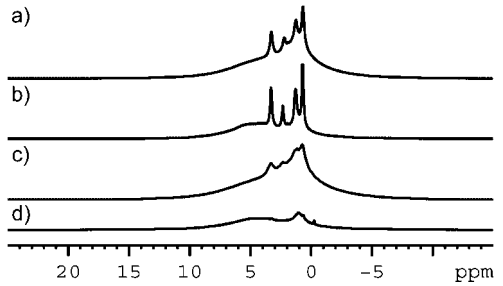

Figure 5. ^{1}H MAS spectra recorded with a spinning rate of 30 kHz. (a) Modification **1a**; (b) **2a** (with CD_3 groups); (c) **1c**; (d) **1d**

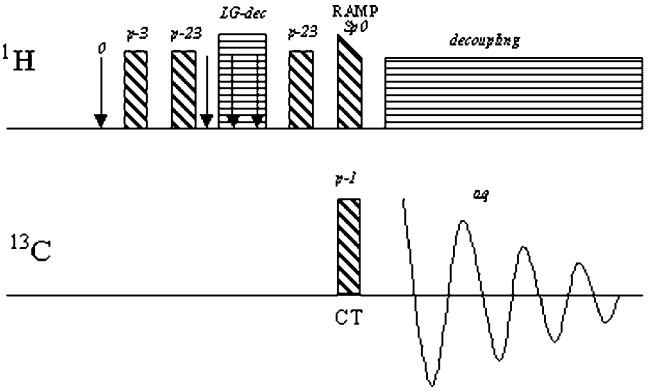

Figure 6. Pulse sequence used for recording of 2D HETCOR spectra; p3 is 90° proton pulse, p23 is 54.7° proton pulse, arrows denote LG offsets, CT is contact time

groups is to the overall spectrum. It is known that methyl groups in the solid state are usually under a fast exchange regime and can be observed as a sharp line.[12] This doubt was explained by employing **2** as host molecule, where the methyl groups are replaced by CD_3 residues. From comparative analysis of liquid-phase ^{1}H NMR spectra of **1** and **2**, the ^{2}H abundance for methyl groups of isopropylidene residues was found to be ∼75%. As can be seen [Fig. 5(b)] the background for **2** is much weaker than that for **1** and resonance lines for *n*-propanol are better split. Figure 5(c) presents the ^{1}H MAS spectrum of **1c** with a long ^{31}P T_1. The differences between spectra are apparent. The linewidth for resonance lines of **1c** is much larger and in consequence the resolution is much worse. Finally, we recorded the ^{1}H MAS spectrum for **1d** without solvent in the crystal lattice. As can be seen, the spectrum is very broad, which clearly proves that the sharp signals observed in Fig. 5(a) and (b) characterize guest molecules in the host cavity.

Finally, we have established ^{1}H T_1 relaxation times for guests employing the inversion–recovery technique. As we found, the T_1 for a guest located in the cavity are slightly longer compared with the case when the guest molecule is probably outside cavity. The corresponding spin–lattice relaxation times are 1.47 and 0.87 s for **1a** and **c**, respectively.

In the next step, we were prompted to answer the question of whether heteronuclear 2D correlation techniques can be used to assign the alignment of a guest in the crystal lattice of the host. For this purpose we employed the ^{1}H–^{13}C frequency switched Lee–Goldburg (FSLG) decoupling experiment (Fig. 6).[13] In FSLG HETCOR, the sample is spun very rapidly, which greatly improves the resolution of carbon and proton projections. Through lengthening of the contact time (CT) in the pulse sequences, it is possible to observe long-range intermolecular interactions. We carried out measurements with six contacts times, 1, 2, 4, 6 and 10 ms, at a spinning rate of 25 kHz and a temperature of 278 K. With the shortest contact time we monitored cross peaks which belong to the *n*-propanol molecule. The relatively weak intensity of methyl group due to the well-known small efficiency of cross polarization for rotating groups is noteworthy.[14]

In order to simplify the interpretation of the spectra, we used an IC with **2** as host. Figure 7(a) shows the 2D correlation for the **2a** IC with a contact time of 6 ms. Of course, for apparent reasons the resolution in the F_1 projection is not as good as for the ^{1}H–^{13}C HSQC spectrum measured in the liquid phase (see Supplementary material); however, some structural information can be gained. The cross peak between protons of the methyl group of the guest and methyls of the isopropylidene residue is evident. The other cross peaks showing the

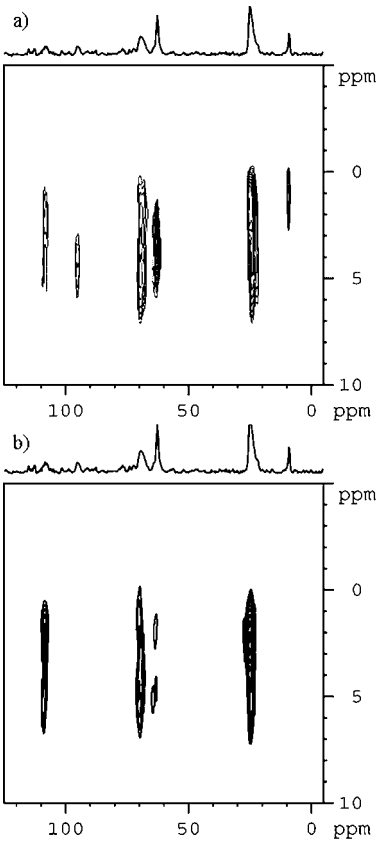

Figure 7. ^{1}H–^{13}C FSLG HETCOR MAS spectra of (a) **2a** and (b) **2c** recorded with a spinning rate of 25 kHz

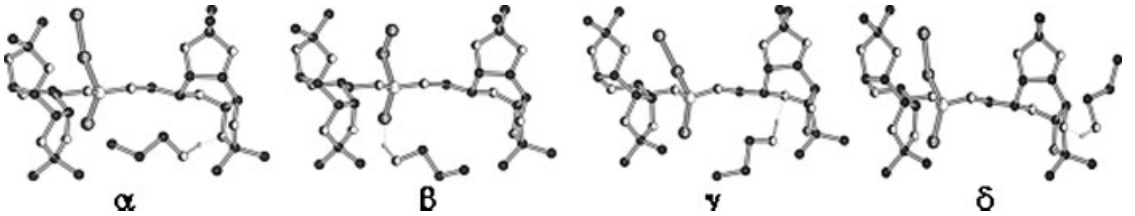

Chart 2

short-range correlation for both guest and host molecules are clearly seen. The important structural constraint is presence of a long-range cross peak between residual protons of the methyl groups of isopropylidene and quaternary carbons. The most significant information was obtained on searching the region of the anomeric signal at 97 ppm. The cross peak for the C1 carbon is in an unexpected region. From the HSQC correlation, we predicted the presence of the ^{1}H signal at 5.5 ppm in the F_1 dimension. The signal observed at $\sim$4 ppm (F_1 projection) may be due to intramolecular contact with a CH_2 group (the C1—C6 distance is 3.63 Å) and/or intermolecular interaction with the —CH_2(1)— proton of the guest molecule [see Fig. 4(b)]. Further results were obtained for **2c**. Figure 7(b) shows the FSLG HETCOR spectrum recorded with CT 6 ms and other experimental parameters as for **2a**. The difference between Fig. 7(a) and (b) is apparent. The lack of the cross peak for anomeric carbon in Fig. 7(b) suggests that in the former case the cross peak rather reflects host–guest interactions and very likely for **2c** *n*-propanol is outside the cavity. The signals that correspond to the guest molecule in the crystal lattice are much weaker in Fig. 7(b) than in Fig. 7(a). The methyl group is not seen in the 2D projection. On the other hand, the ^{1}H NMR studies in the liquid phase unambiguously prove that for both samples the quantity of guest in the ICs is exactly the same. In the FSLG HETCOR experiment, for each sample, even with very long CT, we did not monitor a C1–H1 host cross peak corresponding to the closest intramolecular contact. This means that the proton signal of the anomeric group is very broad, hidden in the baseline, which causes that C–H intramolecular interaction not to be detected. Finally, it is worth stressing that analysis of the cross-polarization profiles for **2a** and **c** in the CT range from 10 µs to 12 ms did not reveal a distinction in the ^{1}H $T_{1\rho}$ relaxation times for anomeric carbons. Hence the difference between 2D spectra is not due to distinction of the cross-polarization dynamics of **2a** and **c**.

DFT calculations

In order to have better insight into the structure of the ICs of **1**, in the next step we carried out density functional theory (DFT) calculations.[15] Theoretical methods have recently become an attractive approach to search for various possible geometries of host–guest compounds.[16] The host molecule of **1** is a species in which the cavity has few sites that can be considered as hydrogen bond acceptors. From x-ray studies, it is apparent that hydrogen bonding occurs between *n*-propanol and the oxygen of the isopropylidene blocking group. Such a structure, labeled case **α** in Chart 2, was considered as a starting point in our calculations. We also built up a structure where thiono-sulfur is a hydrogen bond acceptor (case **β**). It is worth emphasizing that such a geometry was established by means of x-ray diffraction for the inclusion complex of **1** with 2-propanol.[17] Moreover, structures **γ** and **δ** have been taken into consideration. In each case, the crystal structure of the host molecule was taken as the starting geometry. The position of the hydrogen atoms of **1** was optimized at the PM3 level since x-ray diffraction often has difficulty locating protons accurately.

In all calculations, the geometry of host was 'frozen' and the distance between heavy atoms of the hydrogen bridge (S or O) was kept in the region of 3.2 Å as found in x-ray structures. For **β** and **δ** structures the alignment of *n*-propanol was optimized. In each case the guest was considered as a static molecule although from the experiment it is clear that at room temperature *n*-propanol undergoes reorientation. With these precautions, DFT calculations at the B3PW91/6–311 + G* level were carried out.[18] The calculated energies for modifications **α**–**ε** are given in Table 2. From these data, it is clear that localization of the guest molecule in the crystal lattice has a noticeable influence on the global energy of complexes. Structures with *n*-propanol inside the cavity have lower energy, in particular those where oxygen is an acceptor of hydrogen bonding (**α** and **γ**). Complex **δ** with the guest molecule outside the cavity has the highest energy, higher than the solvent-free matrix.

Table 2. SCF energy in arbitrary units (AU) for modifications **α**–**ε**

Sample	**α**	**β**	**γ**	**δ**[a]	**ε**[b]
E (A)U	−4539 8599	−4539 8557	−4539 8605	−4539 8543	−4539 8568

[a] **δ** shows complex with solvent outside cavity.
[b] **ε** (not shown in Chart 2) represents solvent-free host matrix.

DISCUSSION

Experimental data and theoretical calculations enable us to establish the alignment of guest molecules in the crystal lattice of the host and also to construct a model that in pictorial form explains the nature of the changes.

Chart 3 shows the border stages with *exo* and *endo* cavities. The cylinders represent the sugar molecules and the solid lines correspond to the thiophosphoryl skeleton. When the guest molecule is outside the cavity (*exo* case), the ^{31}P T_1 is very long (**1c**, **2c**) and comparable to the solvent-free host **1d**. Samples **1a** and **2a** represent the pure *endo* case, with guest molecule deeply aligned inside the cavity. In consequence the relaxation times are considerably shorter. We further assume that **1b** is a mixture of **1a** and **c**, very likely in the proportions 0.77:0.23. The rearrangement at ambient temperature of **1c**–**1e** and the dramatic change of the spin–lattice relaxation times is very impressive. It is worth noting that during crystallization we found a number of samples that cover a range of ^{31}P relaxation times from 15 to 115 s. Analysis of ^{13}C T_1 for anomeric carbon is another source of structural information. Inspection of the data for **1a** and **2a** (Table 1) reveals a significant difference in the relaxation times for two observed C1 carbons (15.2 and 34.0 s). From x-ray data it is clear that only two of four sugar residues are involved in short contacts with *n*-propanol [Fig. 4(b)]. For other samples the ^{13}C T_1 of the C1 carbons have comparable values. The much longer relaxation times of anomeric carbons for **1d** without solvent in the lattice is worth noting.

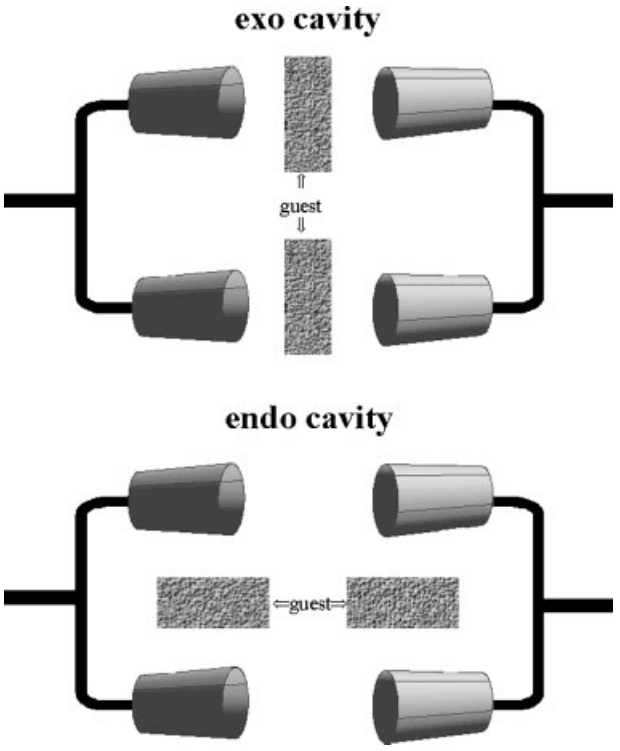

Chart 3

Judging from the changes in DSC profiles, it is plausible that self-organization of ICs causes the subtle crystal lattice modification and release of the guest from the *endo* cavity requires exothermic host recrystallization. Variable-temperature experiments provides further evidence confirming the rearrangement of the host lattice. Figure 8 presents ^{31}P CP/MAS and ^{1}H MAS spectra of **1a** at 65 °C, in the region of exothermic changes [see Fig. 1(a)]. From the ^{31}P spectrum it is apparent that at this temperature the host lattice is changed and we have two components. The ^{1}H MAS spectrum proves that the guest is still in the lattice, but the lineshape is significantly broader than that observed for **1a**. The quantitative liquid-phase ^{1}H NMR measurements show that for both samples, before and after thermal treatment the amount of *n*-propanol in IC is exactly the same. On the other hand, the ^{31}P, ^{13}C and ^{1}H relaxation times are dramatically different. For **1a** after rearrangement appropriate values are very similar to those established for **1c**.

The instability of **1b** and **c** suggests the formation of kinetically controlled products, which undergo rearrangement to the thermodynamically more stable form **1e (1a)**. The thermodynamics of inclusion complexes are well established.[19] Nevertheless, information about the self-organization of ICs under mild conditions is not common. Our experimental and theoretical studies enabled us to establish the mechanism of thermal changes of ICs of **1** and to understand the migration pathway of the guest molecules in the crystal lattice. The crystallization of DGTD in *n*-propanol is a random process with equal probability of forming *exo* and *endo* complexes. It is apparent that weak intermolecular interactions (hydrogen bonding between guest and host molecules) make a very small but important contribution to the total energy of ICs and can be thought of as a driving force which is responsible for the alignment of guest molecules in the 'proper place' in the cavity.

The solid-state NMR measurement of T_1 relaxation times allows the localization of the guest molecules in the lattice to be established. To the best of our knowledge,

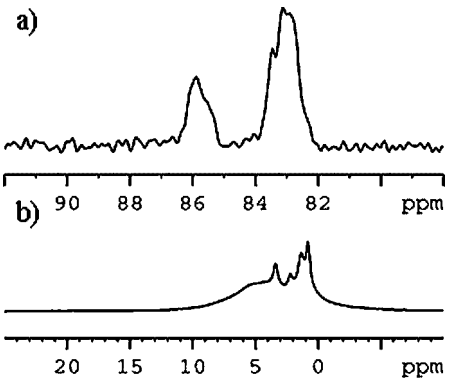

Figure 8. (a) ^{31}P CP/MAS spectrum (only the isotropic part is shown); (b) ^{1}H MAS spectrum for **2a** after heating to 65 °C, recorded with a spinning rate of 30 kHz

this paper presents the first such spectacular example and tools to investigate the self-organization of ICs on macroscopic and molecular levels.

EXPERIMENTAL

Sample synthesis and crystallization. DGTD was synthesized according to procedure described elsewhere.[20] A 100 mg amount of host was dissolved in 20 ml of *n*-propanol by gentle heating. Crystals were grown by slow isothermal evaporation of the solvent over a few days. In most cases when employing this procedure **1a** was obtained. When the solute–solvent mixture after dissolution was quickly cooled, usually crystals of **1c** appeared. However, the crystallization of **1** is random process and in many cases mixtures of different forms are obtained.

NMR measurements. The solid-state ^{1}H, ^{13}C and ^{31}P NMR experiments were performed on a Bruker Avance DSX 300 spectrometer at 300.13 75.47 and 121.49 MHz. The instrument was equipped with a MAS probehead using 4 mm and 2.5 mm ZrO_2 rotors. A sample of glycine was used for setting the Hartmann–Hahn condition and adamantane as a secondary chemical shift reference, $\delta = 38.48$ and 29.46 ppm from external TMS.[21] Phosphoric acid (85%) was used reference for ^{31}P and TMS for ^{1}H spectra. The conventional spectra were recorded with a proton 90° pulse length of 3.5 μs and a contact time of 1 ms. The repetition delay was 10 s and the spectral width was 25 kHz. The FIDs were accumulated with a time domain size of 2K data points. The RAMP shape pulse was used during the cross-polarization and TPPM with $\tau_p = 6.8$ μs and a phase angle of 20° during acquisition.[22,23] The spectral data were processed using the WIN-NMR program.[24]

FSLG HETCOR spectra were recorded with the pulse sequence given in Ref. 13. The 3 μs $\pi/2$ ^{1}H pulse was set up in each 2D experiment. Thirty-two serial files with increment 19.2 μs were recorded. Linear prediction in F_1 was employed. The LG offset was shifted 3 kHz in order to avoid overlap of axial peaks with cross peaks. The spectra were processed with Qsine apodization functions, 2.5 in F_2 and 3 in F_1.

The magnitudes of the principal elements of the CSA were obtained from the best-fitting simulated spinning patterns. Simulations of the spinning CSA sidebands spectra were carried out on a PC using the SIMPSON program under a LINUX environment.

Other methods. DFT GIAO calculations were carried out with the GAUSSIAN 98 program running on a Silicon Graphics Power Challenge computer. The GIAO method with the B3PW91 hybrid method and 6–311++G** basis set was used to calculate geometry and NMR parameters.

DSC and TGA measurements were carried out on TA instruments, 2920 Modulated DSC and Hi-Res TGA 2950 Analyzer.

Acknowledgement

The authors are grateful to the Committee for Scientific Research (MIiN) for financial support, grant No. 3 T09 A 173 27. S. Olejniczak is a Domestic Grants for Young Scientists 'The Foundation for Polish Science' scholarship holder.

REFERENCES

1. Atwood JL. *Inclusion Phenomena and Molecular Recognition*. Kluwer: Dordrecht, 1990.
2. Lehn JM. *Supramolecular Chemistry, Concepts and Perspectives*. VCH: Weinheim, 1995.
3. Steed JW, Atwood JL. *Supramolecular Chemistry.* Wiley: Chichester, 2000.
4. (a) Szejtli J. *Cyclodextrin Technology.* Kluwer: Dordrecht, 1998; (b) Szejtli J. *Chem. Rev.* 1998; **98**: 1743–1753; (c) Crini G. *Prog. Polym. Sci.* 2005; **30**: 38–70; (d) Davis ME, Brewster ME. *Nat. Rev. Drug. Discov.* 2004; **3**: 1023–1035; (e) Del Valle EMM. *Process. Biochem.* 2004; **39**: 1033–1046; (f) Schneiderman E, Stalcup AM. *J. Chromatogr. B* 2000; **745**: 83–102.
5. (a) Allcock HR. *Phosphorus*–Nitrogen Chemistry. Academic Press: New York, 1972; (b) Chandrasekhar V, Krishnan V. *Adv. Inorg. Chem.* 2002; **53**: 159–211; (c) Gleria M, De Jaeger R. *J. Inorg. Organomet. Sci.* 2001; **11**: 1–45; (d) Gleria M, Po R, Giannotta G, Fiocca L, Bertani R, Fambri L, La Mantia FP, Scaffaro R. *Macromol. Symp.* 2003; **196**: 249–270; (e) Gates DP, Manners I. *J. Chem. Soc., Dalton Trans.* 1997; 2525–2532.
6. Potrzebowski MJ, Grossmann G, Ganicz K, Olejniczak S, Ciesielski W, Kozioł AE, Wawrzycka I, Bujacz G, Haeberlen U, Schmitt H. *Chem. Eur. J.* 2002; **8**: 2691–2699.
7. White MA. In *Comprehensive Supramolecular Chemistry*, vol. 8. Atwood JL, Davies JED, MacNicol DD, Vogtle F (eds). Elsevier: New York, 1996.
8. Potrzebowski MJ, Kazmierski S. *Top. Curr. Chem*. 2005; **246**: 91–140.
9. Bak M, Rasmussen JT, Nielsen NC. *J. Magn. Reson*. 2000; **147**: 296–330.
10. Torchia DA. *J. Magn. Reson*. 1978; **30**: 613–616.
11. Comotti A, Gallazzi MC, Simonutti R, Sozzani P. *Chem. Mater.* 1998; **10**: 3589–3596.
12. Straus SK, Bremi T, Ernst RR. *J. Biomed. NMR* 1997; **10**: 119–128.
13. van Rossum BJ, Forster H, de Groot HJM. *J. Magn. Reson*. 1997; **124**: 516–519.
14. Zilm KW. In *Encyclopedia of NMR* (vol. VII), Grant DM, Harris RK (eds). Wiley: Chichester, 1996, and references cited therein.
15. Malkin VG, Malkina OL, Eriksson LA, Salahub DR. In *Theoretical and Computational Chemistry* (vol. 2), Seminaro JM, Politzer P (eds). Elsevier: Amsterdam, 1995.
16. (a) Schatz J, Bakes AC, Siehl H-U. *J. Chem. Soc., Perkin Trans. 2* 2000; 609–610; (b) Bakes AC, Schatz J, Siehl H-U. *J. Chem. Soc., Perkin Trans. 2* 2002; 484–488.
17. Potrzebowski MJ, Blaszczyk J, Wieczorek MW. *J. Org. Chem*. 1995; **60**: 2549–2562.
18. Frisch MJ, Trucks GW, Schlegel HB, Scuseria GE, Robb MA, Cheeseman JR, Zakrzewski VG, Montgomery JA Jr, Stratmann RE, Burant JC, Dapprich S, Millam JM, Daniels AD, Kudin KN, Strain MC, Farkas O, Tomasi J, Barone V, Cossi M, Cammi R, Mennucci B, Pomelli C, Adamo C, Clifford S, Ochterski J, Petersson GA, Ayala PY, Cui Q, Morokuma K, Malick DK, Rabuck AD, Raghavachari K, Foresman JB, Cioslowski J, Ortiz

JV, Stefanov BB, Liu G, Liashenko A, Piskorz P, Komaromi I, Gomperts R, Martin RL, Fox DJ, Keith T, Al-Laham MA, Peng CY, Nanayakkara A, Gonzalez C, Challacombe M, Gill PMW, Johnson B, Chen W, Wong MW, Andres JL, Gonzalez C, Head-Gordon M, Replogle ES Pople JA. *Gaussian 98, Revision A.6*. Gaussian: Pittsburgh, PA, 1998.
19. Rekharsky MV, Inoue Y. *Chem. Rev.* 1998; **98**: 1875–1917, and references cited therein.
20. Potrzebowski MJ, Ganicz K, Ciesielski W, Skowrońska A, Wieczorek MW, Błaszczyk J, Majzner W. *J. Chem. Soc., Perkin Trans. 2* 1999; 2163–2170.
21. Morcombe CR, Zilm KW. *J. Magn. Reson.* 2003; **162**: 479–486.
22. Metz G, Wu X, Smith SO. *J. Magn. Reson. A* 1994; **110**: 219–227.
23. Bennett AW, Rienstra CM, Auger M, Lakshmi KV, Griffin RG. *J. Chem. Phys.* 1995; **103**: 6951–6958.
24. *Win-NMR, Version 6.0*. Bruker-Franzen Analytik: Bremen, 1993.